Doppler effects of a light source on a metamaterial slab: a rigorous Green's function approach

Weihua Wang,[1] Xueqin Huang,[1] Lei Zhou,[1,*] and C. T. Chan[2]

[1]*Surface Physics Laboratory and Physics Department, Fudan University, Shanghai 200433, China*
[2]*Physics Department, Hong Kong University of Science and Technology, Clear Water Bay, Kowloon, Hong Kong, China*
**Corresponding author: phzhou@fudan.edu.cn*

Received October 12, 2007; revised January 10, 2008; accepted January 14, 2008; posted January 22, 2008 (Doc. ID 88512); published February 14, 2008

We apply a (rigorous) Green's function theory to study the Doppler effects of a light source placed on top of a metamaterial slab. When the receiver is in motion with the source and the slab, we find that, in addition to a conventional Doppler mode, there are several other frequency components that do not obey the standard frequency-shift rule. We show that such new effects are caused by the coupling between the radiated electromagnetic waves and the surface modes of the metamaterial slab, whose dispersion relation varies as a function of velocity in the moving reference frame. © 2008 Optical Society of America

OCIS codes: 260.2110, 160.3918.

Doppler effects, a fundamental property of all waves [electromagnetic (EM), sound, etc.], are the phenomena in which the received signal possesses an enhanced (decreased) frequency compared with the radiated one when the source and receiver approach (move away from) each other [1]. In 1968, Veselago predicted that the Doppler shift will be reversed if the source and receiver are embedded in a negative-index medium [2]. People then realized that such inverse Doppler effects could also occur in other media, such as plasmas [3], photonic crystals [4], or transmission lines [5,6], inside which the wave dispersions are strongly modified. Recently, Doppler signals were observed even when the moving source's working frequency was inside a forbidden gap [7,8].

We note that previous theoretical treatments [4,7,8] typically employed a Galilean transformation to consider the movements of the source or receiver. In this Letter, we apply a rigorous Green's function theory, in which a Lorentz transformation is employed and the emitter is taken as a realistic line current source, to study the Doppler effects when the source and the receiver are both placed on top of a metamaterial slab and are in relative motion with respect to each other. Beside a conventional Doppler mode, we find several other frequency components that do not obey the standard frequency shift rule. We find that such new effects are caused by coupling between the radiated EM waves and the surface modes of the metamaterial slab, whose dispersion is drastically changed in the moving receiver's reference frame.

The geometry of our system is schematically shown in Fig. 1, where a line current source and a point receiver, both placed on top of a metamaterial slab of thickness d and with a widely adopted response function $\epsilon_r(\omega)=\mu_r(\omega)=1-\omega_p^2/\omega(\omega+i\delta)$ [9], are moving at velocities $v_s\hat{x}$ and $v_r\hat{x}$ with respect to the slab. We define three reference frames, denoted the S', S, and $\tilde{S}$ frames, inside which the source, slab, and receiver are at rest, respectively. A line source, working at an angular frequency ω_0 with the simplest switch-on process, takes a form $\vec{J}'(\vec{r}',t')=\hat{y}I_0\delta(x')\delta(z')e^{-i\omega_0 t'}\theta(t')$ in the S' frame. Employing the Lorentz transformation [1], we find that the source takes the form $\vec{J}(\vec{r},t)=\hat{y}I_0\delta(\gamma_s x-\gamma\beta_s ct)\delta(z)e^{-i\omega_0\gamma_s(t-\beta_s x/c)}\theta[\gamma_s(t-\beta_s x/c)]$ in the S frame, where $\beta_s=v_s/c$, $\gamma_s=1/\sqrt{1-\beta_s^2}$ and c is the speed of light in vacuum. The EM fields in the S frame can be exactly calculated in terms of $\vec{J}(\vec{r},t)$, following the dyadic Green's function theory [10,11]. We then perform the Lorentz transformation [1], $\tilde{E}_x=E_x$, $\tilde{E}_y=\gamma_r(E_y-v_rB_z)$, $\tilde{E}_z=\gamma_r(E_z+v_rB_y)$, $\tilde{B}_x=B_x$, $\tilde{B}_y=\gamma_r(B_y+\beta_rE_z/c)$, $\tilde{B}_z=\gamma_r(B_z-\beta_rE_y/c)$, with $\beta_r=v_r/c$, $\gamma_r=1/\sqrt{1-\beta_r^2}$, to calculate the EM fields in the $\tilde{S}$ frame, which are the signals measured by the receiver. We finally perform a Fourier transform, $\tilde{\vec{E}}(\tilde{\vec{r}},\tilde{\omega})=\int e^{i\tilde{\omega}\tilde{t}}\tilde{\vec{E}}(\tilde{\vec{r}},\tilde{t})\mathrm{d}\tilde{t}$, to get the frequency spectrum of the received signal. For example, a straightforward calculation shows that

$$\tilde{E}_y(\tilde{\vec{r}},\tilde{\omega})=-\frac{i\mu_0 I_0}{4\pi}\int\frac{\gamma_r\tilde{\omega}}{\gamma_s\tilde{\omega}-\gamma_r\omega_0+\gamma_s\gamma_r^2(c\tilde{k}_x+\beta_r\tilde{\omega})(\beta_r-\beta_s)+i\gamma_r\eta\,\tilde{k}_{0z}}\frac{e^{i\tilde{k}_x\tilde{x}}}{\tilde{k}_{0z}}(e^{-i\tilde{k}_{0z}\tilde{z}}+\tilde{R}^{\mathrm{TE}}e^{i\tilde{k}_{0z}\tilde{z}})\mathrm{d}\tilde{k}_x,\tag{1}$$

where $\tilde{k}_{0z}=\sqrt{(\tilde{\omega}/c)^2-\tilde{k}_x^2}$ and $\tilde{R}^{\mathrm{TE}}(\tilde{\omega},\tilde{k}_x)$ is the reflection coefficient measured in the $\tilde{S}$ frame when a transverse-electric (TE) polarized plane wave with frequency $\tilde{\omega}$ and parallel wave vector $\tilde{k}_x$ strikes the metamaterial slab. Specifically, $\tilde{R}^{\mathrm{TE}}(\tilde{\omega},\tilde{k}_x)=e^{-i\tilde{k}_{0z}2d}[(1-\tilde{\Delta}^2)e^{-i\tilde{k}_{1z}d}-(1-\tilde{\Delta}^2)e^{i\tilde{k}_{1z}d}]/[(\tilde{\Delta}+1)^2e^{-i\tilde{k}_{1z}d}$

0146-9592/08/040369-3/$15.00

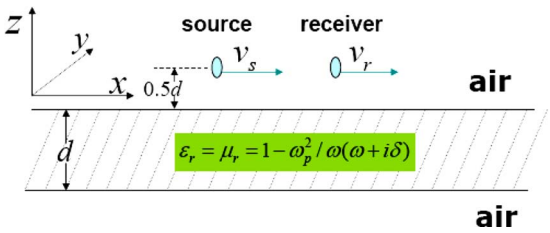

Fig. 1. (Color online) Geometry of the system studied in this paper. At $t=0$, the source and receiver are located at (0,0,0) and $(0.1d,0,0)$.

$-(\tilde{\Delta}-1)^2 e^{i\tilde{k}_{1z}d}]$ [12], with $\tilde{\Delta}=\tilde{k}_{1z}/(\tilde{k}_{0z}\tilde{\mu}_r)$, and $\tilde{k}_{1z}=\sqrt{\tilde{\epsilon}_r\tilde{\mu}_r\cdot[\gamma_r(\tilde{\omega}/c+\beta_r\tilde{k}_x)]^2-[\gamma_r(\tilde{k}_x+\beta_r\tilde{\omega}/c)]^2}$. Here the permittivity and permeability in the moving $\tilde{S}$ frame are given by

$$\tilde{\epsilon}_r = \epsilon_r(\gamma_r\tilde{\omega} + \gamma_r v_r\tilde{k}_x), \tilde{\mu}_r = \mu_r(\gamma_r\tilde{\omega} + \gamma_r v_r\tilde{k}_x). \quad (2)$$

We note that these response functions become spatially nonlocal in the moving $\tilde{S}$ frame, as long as the metamaterial is dispersive [13].

As a test, we first study the Doppler effects in vacuum [i.e., we set $\tilde{R}^{\mathrm{TE}}\equiv 0$ in Eq. (1)]. Obviously, $\tilde{\omega}_r$ of the received signal corresponds to a peak in function $\tilde{E}_y(\tilde{\omega})$. Owing to the integration over $\tilde{k}_x$ in Eq. (1), we expect $\tilde{\omega}_r$ to make the two denominators zero simultaneously, leading to a solution

$$\tilde{\omega}_r = \omega_0\gamma_r(1-\beta_r)/[\gamma_s(1-\beta_s)]. \quad (3)$$

We note that Eq. (3) describes the classical Doppler effect generally [14]. Numerical calculations based on Eq. (1) confirmed the above arguments. For simplicity, we assume the source to be at rest ($v_s\equiv 0$) throughout this work. As shown in Fig. 2(a), we find that the peak in the spectrum calculated for $v_r=0.01c$ (dotted curve) is downshifted compared with that obtained at $v_r=0$ (solid curve), and the frequency shift agrees well with that predicted by Eq. (3).

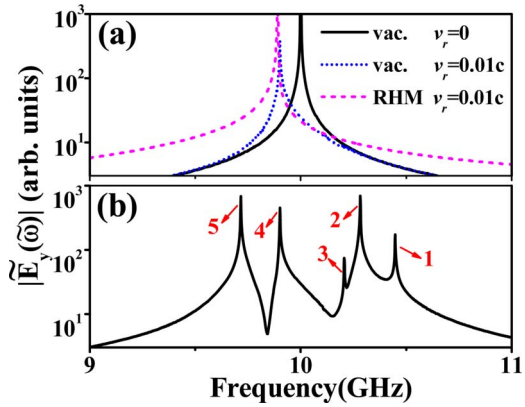

Fig. 2. (Color online) (a) Frequency spectra measured by a receiver in vacuum at rest (solid) or with $v_r=0.01c$ in vacuum (dotted), and by a moving receiver on top of a normal right-handed material (RHM) layer (dashed). (b) Frequency spectrum measured by a receiver moving with $v_r=0.01c$ on top of a metamaterial slab.

We now study the Doppler effects in the presence of a metamaterial slab. Assuming that $\omega_p=20\sqrt{2}\pi$ GHz, $\omega_0=20\pi$ GHz, $\delta=0.006$ GHz, $d=10$ mm, and $v_r=0.01c$ [9], we numerically evaluated $\tilde{E}_y(\tilde{\omega})$ based on Eq. (1), and we show the result in Fig. 2(b). Surprisingly, we find that the spectrum contains five peaks, inside which the fourth one can be identified as the classical Doppler mode. Obviously, such new effects must be due to the metamaterial slab, since the spectrum measured in the presence of an ordinary slab (with $\epsilon_r=1.5$) of the same thickness does not possess such additional peaks [see the dashed curve in Fig. 2(a)].

Such anomalous modes possess many unusual properties. Equation (3) indicates that the Doppler mode is dependent on both ω_0 and v_r. However, Fig. 3 shows that the frequencies of those anomalous modes are almost independent of ω_0, although the classical Doppler mode exhibits a linear dependence on ω_0. The v_r dependences of those additional modes are also quite unusual. From Fig. 4, where the frequency shifts are depicted versus v_r for all five modes, we again find that only the fourth mode satisfies the standard rule and the remaining modes behave anomalously. For example, the frequency shifts for the first two modes show reversed v_r dependences, resembling the inverse Doppler effects [4–8], and the other two show enhanced v_r dependences compared with the classical Doppler mode.

Analyzing Eq. (1) indicates that only a diverging $\tilde{R}^{\mathrm{TE}}$ generates an additional peak in the spectrum function. Since $\tilde{R}^{\mathrm{TE}}(\tilde{\omega},\tilde{k}_x)$ is the reflection coefficient of the slab, such divergences must correspond to the surface wave (SW) excitations of the slab [15]. We calculated the SW dispersion relation by setting the denominator of $\tilde{R}^{\mathrm{TE}}(\tilde{\omega},\tilde{k}_x)$ to zero and depicted the dispersion in Fig. 5(a) as open circles, which are bounded outside two light lines satisfying $(\tilde{\omega}_r/c)^2=\tilde{k}_x^2$. Compared with the dispersion calculated in the static-slab frame [16], here the dispersion in the moving frame is distorted and becomes asymmetric for $\pm\tilde{k}_x$. This is because $\tilde{\epsilon}_r$, $\tilde{\mu}_r$ vary as the functions of velocity and become dependent on $\tilde{k}_x$ in the moving

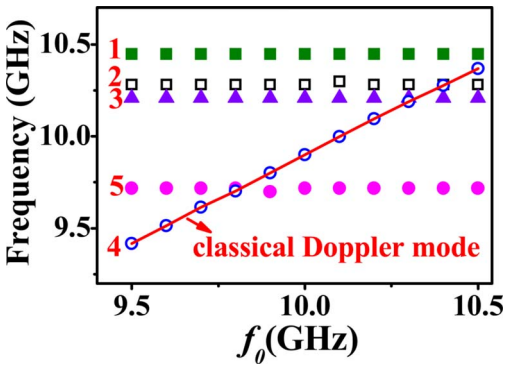

Fig. 3. (Color online) Frequencies of all five modes inside the received signal as functions of the source's working frequency f_0, with the solid line representing the standard Doppler shift rule. Here, $v_r=0.01c$.

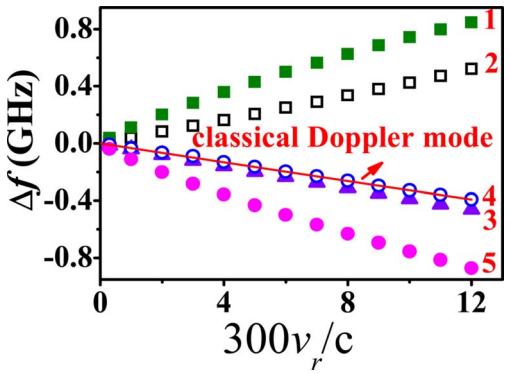

Fig. 4. (Color online) Frequency shifts $\Delta f=[\tilde{\omega}_r(v_r)-\tilde{\omega}_r(0)]/2\pi$ of different modes as functions of v_r, with the solid line representing the standard Doppler shift rule. Here, $f_0=10$ GHz.

frame [see Eqs. (2)]. The distorted dispersion contains four frequencies at which the SW group velocities ($v_g=\partial\tilde{\omega}/\partial\tilde{k}_x$) are zero, and in turn the SW density of states (DOS) diverge. These high-DOS states can be traced back to the edge state and the $\epsilon=\mu=-1$ state [16,17], which are degenerate for $\pm\tilde{k}_x$ in the static-slab frame.

Figure 5(a) offers us a unified picture for understanding all predicted phenomena. Consider first the classical Doppler mode. The solid line in Fig. 5(a) represents the solution of $\tilde{\omega}=\omega_0/\gamma_r-v_r\tilde{k}_x$ [the divergence of the first term in Eq. (1)], which is understood as the source spectrum function seen in the $\tilde{S}$ frame [18]. The classical Doppler mode corresponds to a cross point between the source spectrum and the light line [19]. Since the source always contains a switch-on process, transient components are inevitable, and they are coupled to the SW states of the slab. The strengths of such coupled modes are proportional to the DOS of the slab SWs, so that only the modes at frequencies with divergent SW DOS are dominant. These coupled modes were collected by the receiver as pronounced signals. Comparison between the SW dispersion and the calculated $\tilde{E}_y(\tilde{\omega})$ [Fig. 5(b)] validates the above picture. The reversed velocity dependence is also understandable. In the moving frame, the edge state and the $\epsilon=\mu=-1$ state each split into a pair of states (with $\tilde{k}_x$ and $-\tilde{k}_x$), and the splitting becomes larger as v_r increases. Thus states with positive $\tilde{k}_x$ must have opposite v_r dependences compared with those with negative $\tilde{k}_x$.

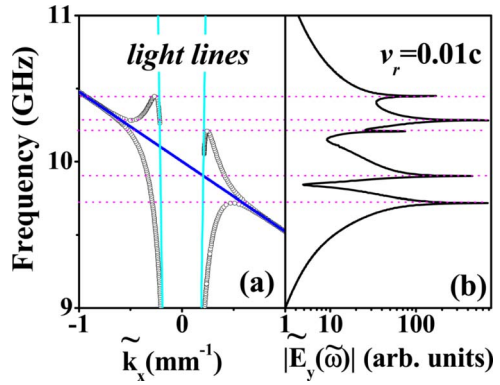

Fig. 5. (Color online) (a) SW dispersion relation (open circles) of the metamaterial slab measured in the receiver's frame, with the thick solid line representing the source's spectrum $\tilde{\omega}=\omega_0/\gamma_r-v_r\tilde{k}_x$. (b) Calculated frequency spectrum of the received signal. Here, $v_r=0.01c$.

In short, we employed a rigorous approach to study the Doppler effects of a line source on a metamaterial slab and found anomalous Doppler modes caused by the coupling between transient waves and the slab surface modes.

This work was supported by the China-973 program, the Natural Science Foundation of China FYTEF, and PCSIRT. C. T. Chan was supported by Hong Kong Central Allocation grant HKUST3/06C.

References and Notes

1. J. A. Kong, *Electromagnetic Wave Theory* (Higher Education, 2002).
2. V. G. Veselago, Sov. Phys. Usp. **10**, 509 (1968).
3. M. Einat and E. Jerby, Phys. Rev. E **56**, 5996 (1997).
4. E. J. Reed, M. Soljačić, and J. D. Joannopoulos, Phys. Rev. Lett. **91**, 133901 (2003).
5. N. Seddon and T. Bearpark, Science **302**, 1537 (2003).
6. A. B. Kozyrev and D. W. von der Weide, Phys. Rev. Lett. **94**, 203902 (2005).
7. X. H. Hu, Z. H. Hang, J. Li, J. Zi, and C. T. Chan, Phys. Rev. E **73**, 015602 (2006).
8. C. Y. Luo, M. Ibanescu, E. J. Reed, S. G. Johnson, and J. D. Joannopoulos, Phys. Rev. Lett. **96**, 043903 (2006).
9. Qualitative conclusions reported here are not affected by the specific forms of $\epsilon_r(\omega)$, $\mu_r(\omega)$, and the parameters are chosen only for easy illustration. Given the velocity adopted in this paper, we find that calculations based on a Galilean transformation do not lead to a significantly different result.
10. L. Zhou, X. Q. Huang, and C. T. Chan, Photonics Nanostruct. Fundam. Appl. **3**, 100 (2005).
11. Y. Zhang, T. M. Grzegorzyk, and J. A. Kong, Electromagn. Waves **35**, 271 (2002).
12. $\tilde{R}^{\mathrm{TE}}(\tilde{\omega},\tilde{k}_x)$ is obtained by applying a Lorentz transformation to $R^{\mathrm{TE}}(\omega,k_x)$, the reflection coefficient calculated in the static-slab frame following [11].
13. In the static-slab frame, $\vec{D}(\vec{r},t)$ is determined by $\vec{E}(\vec{r},t')$, as the response is spatially local. However, after the Lorentz transformation in a moving frame, the point $\{\vec{r},t\}$ is spatially different from the point $\{\vec{r},t'\}$ as long as $t\neq t'$, so that the response appears spatially nonlocal.
14. We get $\tilde{\omega}_r=\omega_0\sqrt{(1+\beta_s)/(1-\beta_s)}$ when $v_r=0$ and $\tilde{\omega}_r=\omega_0\sqrt{(1-\beta_r)/(1+\beta_r)}$ when $v_s=0$. The frequency shift is zero ($\tilde{\omega}_r=\omega_0$) when $\beta_s=\beta_r$.
15. R. Ruppin, J. Phys. Condens. Matter **13**, 1811 (2001).
16. X. Q. Huang, L. Zhou, and C. T. Chan, Phys. Rev. B **74**, 045123 (2006).
17. We note that such states had been observed experimentally, see R. B. Pettit, J. Silcox, and R. Vincent, Phys. Rev. B **11**, 3116 (1975).
18. The spectrum is reduced to $\tilde{\omega}=\omega_0$ when $v_r=0$.
19. Another cross point is automatically excluded in the calculations by the causality requirement.